

Hamming Attention Distillation: Binarizing Keys and Queries for Efficient Long-Context Transformers

Mark Horton¹, Tergel Molom-Ochir¹, Peter Liu¹, Bhavna Gopal¹, Chiyue Wei¹,
Cong Guo¹, Brady Taylor¹, Deliang Fan², Shan X. Wang³, Hai Li¹, and Yiran Chen¹

¹Duke University

²Arizona State University

³Stanford University

{mark.horton, tergel.molom-ochir, peter.liu, bhavna.gopal, chiyue.wei, cong.guo, brady.g.taylor, hai.li, yiran.chen}@duke.edu, dfan@asu.edu, sxwang@stanford.edu

Abstract

Pre-trained transformer models with extended context windows are notoriously expensive to run at scale, often limiting real-world deployment due to their high computational and memory requirements. In this paper, we introduce Hamming Attention Distillation (HAD), a novel framework that binarizes keys and queries in the attention mechanism to achieve significant efficiency gains. By converting keys and queries into -1, +1 vectors and replacing dot-product operations with efficient Hamming distance computations, our method drastically reduces computational overhead. Additionally, we incorporate attention matrix sparsification to prune low-impact activations, which further reduces the cost of processing long-context sequences.

Despite these aggressive compression strategies, our distilled approach preserves a high degree of representational power, leading to substantially improved accuracy compared to prior transformer binarization methods. We evaluate HAD on a range of tasks and models, including the GLUE benchmark, ImageNet, and QuALITY, demonstrating state-of-the-art performance among binarized Transformers while drastically reducing the computational costs of long-context inference.

We implement HAD in custom hardware simulations, demonstrating superior performance characteristics compared to a custom hardware implementation of standard attention. HAD achieves just **1.78%** performance losses on GLUE compared to 9.08% in state-of-the-art binarization work, and **2.5%** performance losses on ImageNet compared to 12.14%, all while targeting custom hardware with a **79%** area reduction and **87%** power reduction compared to its standard attention counterpart.

1 Introduction

Since the introduction of the transformer [32], various adaptations of the architecture have spread across nearly every domain of deep learning, achieving state-of-the-art performance

across modalities such as language, vision, video, and audio [7; 8; 2; 33]. The versatility and success of the transformer is largely attributable to its self-attention module, which learns pairwise relationships and information sharing between vectors in its set of inputs, each of which can represent language tokens, image patches, etc. While this provides a flexible approach to learn relationships in complex data, the pairwise operations also result in $O(n^2)$ runtime, where n is the number of inputs to the self-attention module. This means that when processing a text, we would expect the runtime to scale with the square of the length of the text, while all other operations in the transformer scale linearly to the length of the text as visualized in Figure 1.

This poor scaling is a critical bottleneck across many fields where we may want to apply transformers. Chatbots processing very long texts for question answering, LLM-based search tools processing a large number of web pages, vision transformers applied to large and high-resolution images, and video models all demand context lengths past what standard transformers can efficiently accommodate. This has led to a large research literature on alternatives for self-attention with better asymptotic scaling, targeting long-context settings [10; 37; 34]. However, none of these approaches has overtaken standard self-attention in popularity for a number of reasons from accuracy/performance losses to poor hardware utilization and throughput. Additionally, many of these approaches cannot be easily used to adapt an existing pre-trained transformer for long-context inference.

Binarization, a special case of quantization, is another research area which has sought to improve the runtime and performance characteristics of deep neural networks. However, unlike the long context literature which focuses on asymptotic runtime advantages, the binarization literature focuses on efficiently leveraging hardware. This is done by replacing floating point weights and activations with binary values, therefore replacing expensive floating point operations with far more memory and runtime efficient bitwise operations. These approaches often target custom hardware [20] designed to run neural networks on edge devices at the cost of some performance loss.

Currently, hardware development is moving past only targeting edge devices and into the server farm, where deep

learning architectures such as transformers have become so massive, slow, and energy intensive as to demand custom hardware solutions. This has led to cutting edge accelerators such as the Google TPU [14], Cerebras CS-2 [21], and Groq TSP [1] among others. This development opens the door to new approaches in algorithm development. Conventionally, binarization techniques would have been focused on lightweight edge devices, making long context applications unrealistic. Additionally, long-context work would be constrained to target conventional GPU hardware, which is optimized for dense, floating point arithmetic. Our work bridges this gap, selectively applying binarization techniques to target custom hardware for efficient long context inference. Our main contributions are as follows:

1. We present a novel, fast, and lightweight framework for fine-tuning transformers to enable binarization of keys and queries and sparsification of the attention matrix, accelerating all $O(n^2)$ attention operations.
2. We evaluate the proposed binarized models across various architectures and tasks, showcasing minimal accuracy degradation.
3. We assess the performance of a binarized model on the QuALITY long-context question answering benchmark [24], demonstrating improved performance with extended context.
4. We simulate the computational efficiency of our binarized attention mechanism on custom hardware, revealing significant performance gains compared to standard attention.

2 Related Work

2.1 Long Context Architectures

A wide range of variations of and replacements for self-attention have been proposed to address the $O(n^2)$ scaling problem. A number of these approaches use fixed, sparse attention maps, with fewer than $O(n^2)$ active elements. For example, longformer [3] combines local dilated and non-dilated sliding-window attention with a fixed number of globally attending tokens, producing an attention matrix with $O(n)$ non-zero elements and fully networked tokens over multiple sequential attention layers. BigBird [37] is similar, but also includes randomly selected non-zero elements in the attention matrix.

Another approach, the Reformer [16], uses locality sensitive hashing to bucket keys and queries, and performs attention within these limited buckets. All of these approaches produce non-trivial accuracy losses against otherwise equivalent models. More recently, Mamba [10] has gained popularity as a competitive attention replacement across many tasks, radically departing from attention and using a state space model instead. While promising, this offers a radically different set of tradeoffs from standard attention, and is even more poorly suited as a drop-in replacement to finetune pre-trained transformers for long context tasks.

Across the long-context field, almost all works focus on asymptotic runtime improvements rather than improving

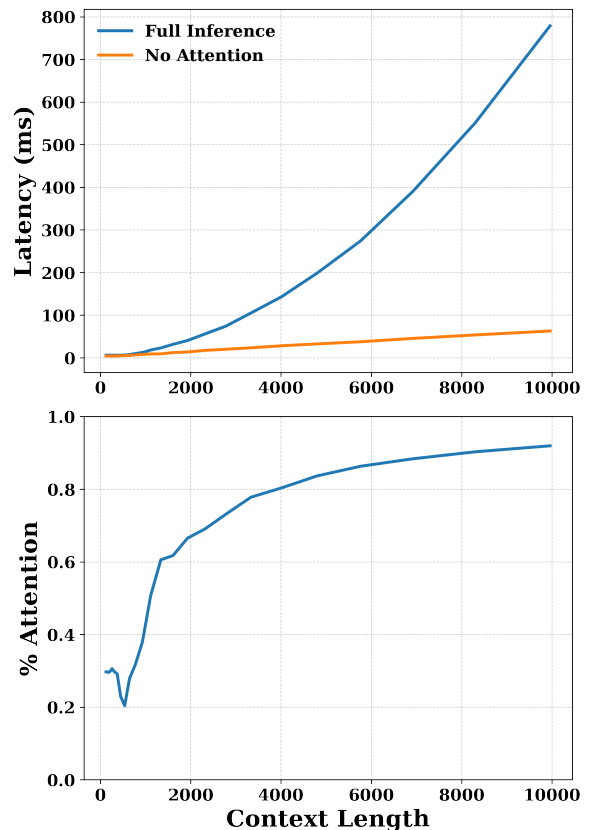


Figure 1: Runtime analysis of BERT Base over increasing context lengths on NVIDIA L40 GPU. As context length rises into the thousands, attention begins to dominate the runtime. The top plot shows the latency of BERT inferred with and without its attention, and the bottom shows the percentage of latency attributable to attention versus all other operations.

hardware utilization, and very few consider adapting pre-trained transformers.

2.2 Deep Neural Network Binarization

Binarized neural networks [13], trained with binary weights and activations, were developed to increase the efficiency of deep neural network inference, and predate the transformer architecture. While early works focused on convolutional neural networks [27], many recent works have adapted binarization techniques to address the transformer architecture. Some of these works use variations of weight binarization while quantizing activations gently or not at all [36; 35]. This achieves very small performance degradation at the cost of increased runtime and memory when compared to full binarization approaches.

These approaches are well suited for decoder-only GPT-style language models, where the quality of generated text is highly sensitive to small changes in the loss value, scaling the number of parameters drastically improves performance, and long contexts are not often necessary. However, these approaches do little to nothing to address the computational costs of attention which dominates in long-context settings,

as attention is an operation only between activations in the form of keys, queries, and values.

Other works, generally applied to BERT-style encoder-only models and vision transformers, perform full binarization including activations and attention, maximizing efficiency at the cost of accuracy. Among the state of the art in this category is BiViT [12], which proposes a novel softmax-aware attention matrix binarization function, achieving significantly higher accuracies than previous fully binarized vision transformers. BiT [23] achieved state-of-the-art results on the GLUE benchmark among fully binarized BERT variants, learning scale and threshold terms during binarization and using a multi-step distillation procedure. Much like BiT, our work includes explicit loss terms so that the fine-tuned student model’s attention map closely replicates the teacher model’s. Effectively all of the above listed works use variations of straight-through-estimators (STEs) to estimate gradients for non-differentiable quantized functions, but HAD also uses transformations of the hyperbolic tangent (tanh) function to smoothly transition from continuous to binarized representations, similar to previous binarization works [17].

Many highly optimized binary multipliers exist, which are tailored to perform XNOR-based computations that reduce area and power while maintaining performance [28; 19; 9]. These multipliers leverage the inherent simplicity of binary operations to enable faster computation with reduced hardware requirements, therefore accelerating binarized neural networks. We would expect binarized attention activations to be particularly valuable, as processing in memory approaches which have been successful in accelerating weight-activation operations [4] are not as easily applied to activation-activation operations in attention, exacerbating its costs.

2.3 Binary Keys and Queries

The selective binarization of keys and queries in this work is primarily inspired by associative memory and Hopfield networks. In hopfield networks, a set of binary vectors or “patterns” are stored and can be queried according to some update rule. Modern hopfield networks [5] are capable of addressing a number of unique patterns scaling exponentially with the number of bits per pattern. “Hopfield networks is all you need” [26] demonstrated that self-attention is effectively a generalization of modern hopfield networks to continuous valued patterns in the forms of keys, addressed by queries. This mapping between attention and binary modern hopfield networks, along with the exponential storage capacity of modern hopfield networks, led us to hypothesize that binarizing specifically our keys and queries would still enable expressive attention lookups to retrieve value vectors.

Additionally, studies of scaling laws of transformer-based LLMs find that performance is tightly coupled to parameter count and training data, and very weakly to model shape [15], indicating that the capacity of the attention mechanism does not determine the capacity of the transformer in many cases. Therefore, we do not expect the capacity loss induced by key and query binarization to significantly reduce model performance.

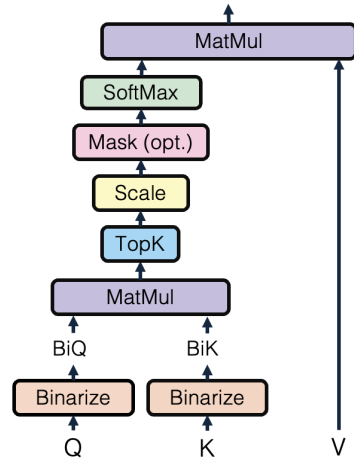


Figure 2: Binarized attention mechanism in Hamming Attention Distillation (HAD), illustrating the binarization of keys (K) and queries (Q) and subsequent attention operations.

2.4 Sparse Attention

Like multiple other works, HAD utilizes a sparse attention matrix. Because the attention matrix is the output of a softmax function, and the relative magnitude of outputs of a softmax is exponential relative to the difference in inputs, large attention matrices contain a large number of near-zero values. Some works such as BigBird [37] and Longformer [3] impose structured sparsity on the attention matrix, with a bias towards nearby elements being able to attend to one another. Other works, exploit the intrinsic sparsity of the attention matrix in order to filter out unwanted features [11] or accelerate transformer inference [22] like HAD.

We select the top N highest attention scores corresponding to each query, and performing a sparse accumulation over our values matrix. While binarization allows us to accelerate the $O(n^2) KQ^T$ operation, sparsity allows us to accelerate the $O(n^2)$ softmax, scaling, and accumulation over V . Many works have proposed GPU and custom hardware solutions, leveraging sparsity to improve efficiency [30; 29].

3 Methods

3.1 Overview

To improve the efficiency of self-attention in long-context scenarios, we propose a novel distillation approach such that given a pre-trained transformer, we can binarize the query (Q) and key (K) matrices and sparsify the attention matrix (A). Our method retains the top N elements of A per query vector, retaining the most relevant attention interactions. We can describe standard attention with the following equations where K , Q , and V are our key, query, and value matrices respectively, A_l is our attention logit matrix, A is our attention matrix, and d_k is the dimension of our attention head:

$$A_l = \frac{QK^\top}{\sqrt{d_k}} \quad (1)$$

$$A = \text{softmax}(A_l) \quad (2)$$

$$\text{Output} = AV \quad (3)$$

In contrast, our modified attention mechanism diagrammed in figure 2 can be described by the following equations where Q_c and K_c are our continuous-valued query and key matrices prior to binarization:

$$Q = \text{sign}(Q_c), \quad K = \text{sign}(K_c) \quad (4)$$

$$A_l = Q \cdot K^\top \quad (5)$$

$$A_{\text{topn}} = \text{topn}(A_l, N) \quad (6)$$

$$A = \text{softmax}(A_{\text{topn}}/\sqrt{d_k}) \quad (7)$$

$$\text{Output} = AV \quad (8)$$

In order to avoid computation on unused attention elements, we perform scaling and softmax and after our top N operation. In order to achieve this binarization, we implement the following multi-stage distillation algorithm.

Algorithm 1 Proposed Training Algorithm

Require: Pre-trained teacher model M_T

Ensure: Optimized student model M_S

- 1: **Initialize:** Copy teacher model weights to student model $M_S \leftarrow M_T$
 - 2: Calculate standardization coefficients σ_Q, σ_K
 - 3: **Stage 1:** Train with scaled tanh approximation, decreasing c from 5 to 1, with A_l distillation loss
 - 4: **Stage 2:** Train with tighter tanh approximation, decreasing c from 1 to 0.05, with A_l distillation loss
 - 5: **Stage 3:** Apply STE-based binarization with A_l distillation loss
 - 6: **Stage 4:** Fine-tune at a lower learning rate without A_l distillation loss
 - 7: **return** Optimized student model M_S
-

In the following sections, we provide a detailed explanation of our approach. Specifically, we cover:

- **Selecting N:** We detail our procedure for selecting our sparsity parameter N .
- **Loss functions:** We define the loss components used during training, including distillation loss and standard training objectives.
- **Standardization coefficients:** A description of the computation of σ_Q and σ_K and their role in binarization.
- **Training stages:** A breakdown of each of the four training stages, detailing their objectives and transition criteria.

3.2 Selecting N

Before we start, we must decide how to set our sparsity parameter N . Figure 3 shows our accuracies distilling a full-precision DeiT tiny model [31] with top N sparsity from its teacher. Starting at $N = 100$ and gradually decreasing, we see accuracy recovery until about $N = 30$ at which point it starts decreasing. DeiT has a context length of 197, and

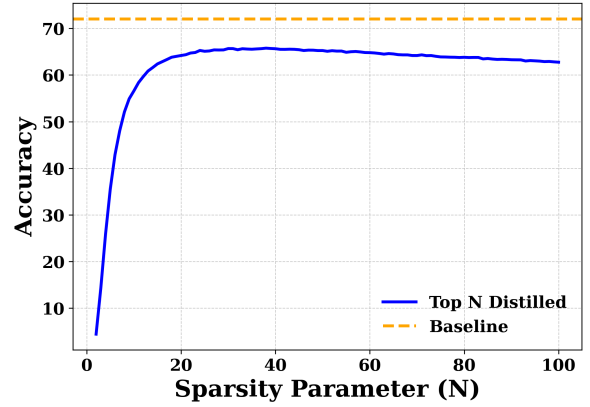


Figure 3: Accuracies measured while progressively distilling a full precision DeiT-T over decreasing N values.

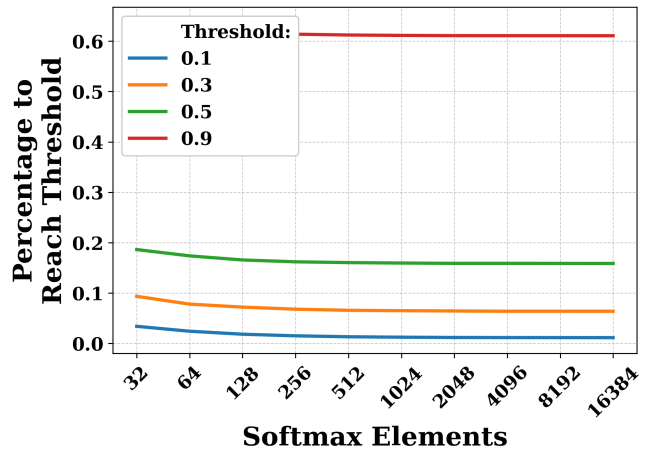


Figure 4: Given standard gaussian inputs, the percentage of the largest softmax outputs required to sum to the threshold probability. In effect, how many elements are required to account for some percentage of probability mass.

we find that $N = 30$ also works well for our BERT models (Section 4.1) [7] with a similar context length of 256 as well as our DeiT models (Section 4.2). However, as we scale to longer contexts, we look to Figure 4 for insights. We find that over larger softmax operations, the percentage of the largest outputs needed to add to some constant probability threshold approaches a constant. We use this as a guiding principle, linearly scaling N with context length in Section 4.3

3.3 Loss Functions

To maintain accuracy after binarization and sparsification, we employ a teacher-student distillation approach. Let $A_{l,t}^{(m)}$ and $A_{l,s}^{(m)}$ represent the attention logit matrices from the teacher and student models, respectively, for attention matrix m . We define the Kullback–Leibler (KL) divergence loss for the attention logits as the unweighted mean over all rows of all attention heads:

$$\mathcal{L}_{\text{KL-att}} = \frac{1}{Mn} \sum_{m=1}^M \sum_{i=1}^n \sum_{j=1}^n \exp(A_{l,t}^{(m)}(i,j)) \left(A_{l,t}^{(m)}(i,j) - A_{l,s}^{(m)}(i,j) \right) \quad (9)$$

where M represents the total number of attention maps (heads · layers), and n represents the number of rows (queries) in each attention map. This formulation encourages the binarized queries and keys, Q and K , to produce attention maps approximating those of their full precision counterparts.

Additionally, we incorporate a KL divergence loss on the model’s output logits, which is defined as:

$$\mathcal{L}_{\text{KL-out}} = \sum_i \exp(z_{t,i}) (z_{t,i} - z_{s,i}) \quad (10)$$

where z_t and z_s are the output logits of the teacher and student models, respectively.

Our final training objective is the sum of the attention and output distillation losses:

$$\mathcal{L} = \mathcal{L}_{\text{KL-att}} + \mathcal{L}_{\text{KL-out}}. \quad (11)$$

3.4 Standardization Coefficients

To facilitate the binarization of the query and key matrices, we estimate the standard deviations σ_Q and σ_K based on the training data.

Our estimation procedure involves performing inference on a subset of the training data. Specifically, we randomly sample 100 minibatches, each containing 16 samples, from the training dataset. For each layer in the model, the standard deviation is computed independently within each minibatch and averaged over all minibatches.

Let $Q^{(b)}$ and $K^{(b)}$ represent the query and key matrices for minibatch b , respectively. The standard deviation for each minibatch is computed as follows:

$$\sigma_Q = \frac{1}{100} \sum_{b=1}^{100} \text{std}(Q^{(b)}), \quad \sigma_K = \frac{1}{100} \sum_{b=1}^{100} \text{std}(K^{(b)}), \quad (12)$$

where $\text{std}(\cdot)$ represents the standard deviation operation applied across all elements within the corresponding matrix.

We find empirically that models such as T5 [25] with K and Q standard deviations far larger or smaller than 1 require standardization with these coefficients for good binarized performance.

3.5 Stage 1: Approaching Tanh

In the first stage of training, we aim to approach a tanh activation for Q and K matrices while preserving essential attention patterns. This is achieved by gradually reducing the scaling parameter c in the binarization approximation function. During stage 1, we apply top N masking to sparsify the attention matrix and employ our combined loss function to guide the training process.

We approximate the binarization of the query and key matrices by using a scaled tanh function. Specifically, the query and key matrices are transformed as follows:

$$Q = c \cdot \sigma_Q \cdot \tanh\left(\frac{Q_c}{c \cdot \sigma_Q}\right), \quad K = c \cdot \sigma_K \cdot \tanh\left(\frac{K_c}{c \cdot \sigma_K}\right), \quad (13)$$

At high c values, this function behaves similar to a linear activation, and at $c = 1$ it behaves similar to tanh scaled by σ . We decay c exponentially from 5.0 until it reaches 1.0, at which point we begin stage 2.

3.6 Stage 2: Approaching Sign

In the second stage of training, we aim to approach a sign activation for Q and K by further reducing the scaling parameter c in the binarization approximation function. Like in stage 1, we apply top N masking and our combined loss function. Our stage 2 transformations are as follows:

$$Q = c \cdot \sigma_Q \cdot \tanh\left(\frac{Q_c}{c \cdot \sigma_Q}\right), \quad K = c \cdot \sigma_K \cdot \tanh\left(\frac{K_c}{c \cdot \sigma_K}\right), \quad (14)$$

We approximate the binarization of the query and key matrices by using a scaled tanh function. Specifically, the query and key matrices are transformed as follows:

$$Q = \sigma_Q \cdot \tanh\left(\frac{Q_c}{c \cdot \sigma_Q}\right), \quad K = \sigma_K \cdot \tanh\left(\frac{K_c}{c \cdot \sigma_K}\right), \quad (15)$$

At $c=1$ this function is equivalent to the end of stage 1, but as it approaches 0 this function approaches the sign function scaled by σ . We continue to decay c exponentially from 1.0 until it reaches 0.05, at which point we begin stage 3.

3.7 Stage 3: Straight-Through-Estimator Training

In stage 3, we aim to refine our binarized K and Q by training with a STE. Once again, we continue to use top N masking and the combined loss. We use the following STE function:

$$\text{STE}_{\text{forward}}(x) = \text{sign}(x), \quad (16)$$

$$\frac{\partial \text{STE}_{\text{forward}}(x)}{\partial x} = \begin{cases} 1, & -1 \leq x \leq 1 \\ 0, & \text{otherwise} \end{cases} \quad (17)$$

which results in the following K and Q transformations:

$$Q = \sigma_Q \cdot \text{STE}\left(\frac{Q_c}{\sigma_Q}\right), \quad K = \sigma_K \cdot \text{STE}\left(\frac{K_c}{\sigma_K}\right) \quad (18)$$

We run this for 10,000 iterations before moving on to stage 4.

3.8 Stage 4: Final Refinement

In stage 4, we use the same binarization function and STE as stage 3. However, we now lower the learning rate and remove the attention map distillation loss, allowing the model more flexibility to adjust its attention maps in service of the output distillation loss:

$$\mathcal{L}(z_t, z_s) = \sum_i \exp(z_{t,i}) (z_{t,i} - z_{s,i}) \quad (19)$$

After 10,000 iterations, we terminate.

3.9 Training Details

All models are distilled with a batch size of 16, the Adam optimizer, a learning rate of 10^{-5} during stages 1-3 and 10^{-6} during stage 4, gradient clipping at magnitude 0.5, and a decay coefficient of 0.9998 per minibatch.

4 Results and Discussion

4.1 GLUE

Table 1 presents results for BERT backbone models distilled and evaluated using the GLUE language understanding benchmark, comparing our approach to BiT [23], which employs full binarization, along with several ablation studies. We observe that by binarizing only the Q and K activations while keeping all other weights and activations in full precision, our method consistently achieves significantly higher accuracies compared to BiT’s full binarization approach. All models used a maximum context length of 256 tokens and all HAD variants used top 30 sparsification of the attention vector per query. All methods seem to significantly struggle with RTE and MRPC, but on all other tasks HAD achieves accuracies within 3% of the baseline teacher model. Notably, we did not face noticeable overfitting issues on any of these tasks, despite running hundreds of distillation epochs for some of the smaller benchmark training datasets.

To further assess the impact of binarizing K and Q versus the attention matrix A, we incorporated the softmax-aware attention binarization (SAB) function and the Straight-Through Estimator (STE) from BiViT [12], while keeping the rest of the training pipeline unchanged (“w/ SAB”). This resulted in substantial accuracy losses. However, this does not necessarily imply that architectures utilizing SAB cannot achieve competitive performance. Rather, it suggests that systems with binarized A may struggle to close the accuracy gap with those using full-precision A and may be highly sensitive to factors such as batch size, training time, and learning rate.

Additionally, we conducted ablation studies by excluding our attention map distillation loss (“w/o AD”) and the tanh training phase (“w/o Tanh”), replacing these with an equivalent number of STE training iterations. We find that both ablations perform comparably to our standard training procedure across many tasks, but yield non-trivial performance losses in some cases. It is worth noting, we observed that attention distillation and tanh binarization contribute significantly when using less optimized training pipelines. We find these techniques add robustness against variations in architectures, tasks, the absence of σ_K and σ_Q normalization, and hyperparameters such as learning rate, batch size, training time, and gradient clipping.

4.2 ImageNet

Table 2 presents results for the base and tiny variants of DeiT [31], distilled and evaluated on the ImageNet [6] image classification benchmark. We once again find that the selective binarization of Q and K produces significantly higher accuracies than implementations including binarization of the attention matrix, as we also saw with the GLUE evaluations. We find that all binarization techniques struggle with the tiny variant of DeiT, indicating that very low capacity attention

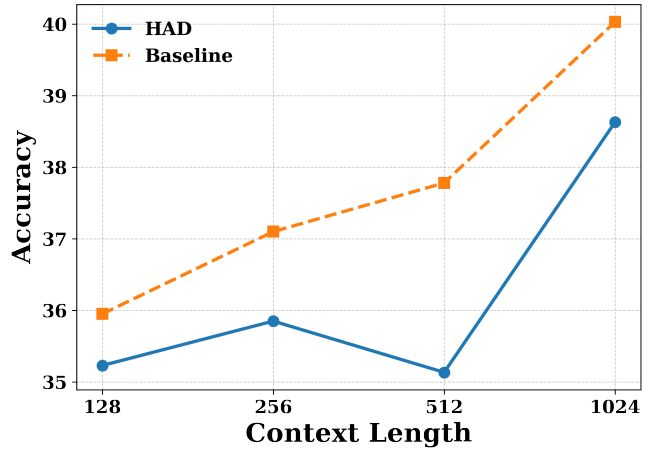


Figure 5: Comparison of HAD and baseline accuracy across different context lengths, evaluated on QuALITY [24]. The context lengths are powers of 2, and the accuracy is measured for both methods.

modules may be disproportionately adversely effected by binarization and/or top N sparsification. When evaluating on ImageNet, the ablations were on par with our full fine-tuning procedure, indicating that these models are less sensitive to attention map distillation and gradual binarization using the STE.

4.3 Long Context Evaluation

To evaluate HAD’s performance in long-context settings, we trained and tested models using the QuALITY long-context multiple-choice question-answering dataset [24] at various context lengths. The QuALITY benchmark contains inputs ranging from 2,000 to 6,000 words, which we truncated to fit the context limits of our models. For our baseline, we used Google’s T5-Base model [25], which was pre-trained on the RACE dataset [18] and fine-tuned on QuALITY truncated to each context length. These truncated QuALITY training data were also used for our distillation dataset.

While our token limits were set to 256 for GLUE and 197 for ImageNet, here we explore context lengths from 128 to 1024 tokens in powers of two. The top N sparsification parameter N was scaled linearly with context length, ranging from 15 at 128 tokens to 120 at 1024 tokens, ensuring a consistent sparsity percentage across experiments.

We observed some noise in accuracies across runs and epochs, which accounts for the performance drop at 512 tokens. However, overall, HAD’s accuracy followed the baseline model’s trend of improvement with increasing context length, achieving within 3% of the baseline model’s accuracy. Combined with our earlier analysis of the softmax function in the long-context regime, these findings support the conclusion that HAD effectively scales to long contexts while maintaining strong performance.

Table 1: GLUE benchmark results comparing our method to the Hugging Face BERT baseline models from TextAttack, BiT, and several ablation studies. "w/ SAB" includes softmax-aware attention map binarization as described in BiViT [12]. "w/o AD" excludes attention map distillation, and "w/o tanh" removes the tanh training stage, replacing it with an equivalent number of STE training steps.

Benchmark	Baseline	HAD (ours)	BiT	w/ SAB	w/o AD	w/o Tanh
MNLI	84.58/84.46	82.45/82.84	79.5/79.4	55.31/56.04	82.00/82.25	82.23/82.58
QQP	90.91	90.11	85.4	78.34	89.51	90.15
QNLI	91.54	89.68	86.4	71.24	89.75	89.64
SST-2	92.43	91.63	89.9	82.34	90.71	90.60
CoLA	53.39	55.47	32.9	16.41	55.82	52.32
STS-B	87.63	87.46	72.0	38.70	86.77	86.78
MRPC	87.75	83.82	79.9	68.87	82.11	83.5
RTE	72.56	65.70	62.1	49.82	64.26	66.06
Avg	82.59	80.81	73.51	57.67	80.13	80.19

Table 2: ImageNet benchmark results comparing our method to the Hugging Face DeiT baseline models from Facebook Research, BiViT, and several ablation studies. "w/ SAB" includes softmax-aware attention map binarization as described in BiViT [12]. "w/o AD" excludes attention map distillation, and "w/o Tanh" removes the tanh training stage, replacing it with an equivalent number of STE training steps.

	DeiT-B	DeiT-T
Baseline	81.74	72.01
HAD (ours)	79.24	66.59
BiViT	69.6	37.9
w/ SAB	6.36	4.32
w/o AD	79.29	66.42
w/o Tanh	79.52	66.78

4.4 Hardware Optimization through Algorithmic Design

To evaluate the impact of algorithmic optimizations on hardware, we synthesized and analyzed a CAM-based binary attention architecture and a conventional BF16 attention design. HAD’s custom design leverages capacitive Content-Addressable Memory (CAM) to replace traditional matrix multiplication in attention mechanisms with in-memory associative matching. Its architecture integrates 1-bit XNOR operations for binarized query-key vectors and employs top N sparsity to significantly reduce power and area. In contrast, the BF16 digital attention showed significantly higher area and power metrics: 31.795 mm² and 25.491 W. Both designs performed attention computation via QK multiplication for $(1 \times 1024) \times (1024 \times 256)$ and Attention Probabilities $\times V$ for $(1 \times 256) \times (256 \times 1024)$. Power and area were estimated using Verilog for a smaller module, synthesized with Synopsys Design Compiler, and scaled to the full design.

5 Conclusion

In this paper, we presented Hamming Attention Distillation (HAD), a novel distillation framework applying selective binarization to address long context transformer inference. HAD selectively binarizes the key (K) and query (Q) projections in transformers while sparsifying the attention matrix.

Table 3: Comparison of Area and Power between Standard Attention (SA) and HAD hardware implementations of an attention head with a context length of 256 and $N = 30$. HAD achieves 79% area and 87% power reduction via CAM-based XNOR operations and sparsity, while maintaining competitive accuracy, highlighting its efficiency over standard attention.

Component	Area (mm ²)		Power (W)	
	SA	HAD	SA	HAD
Q K	15.880	1.108	12.730	0.127
Top N	0.000	0.008	0.000	0.009
SoftMax	0.035	0.017	0.031	0.024
A V	15.880	5.591	12.730	3.141
Total	31.795	6.724	25.491	3.301

By reducing floating point operations, this approach enables highly efficient hardware deployment with a very small performance cost when handling long context inputs. Through distillation, HAD retains strong performance on benchmarks such as GLUE, ImageNet, and QuALITY, while using a fraction of the compute resources of standard attention.

Future work may explore extending our method to efficient GPU implementations, increasing tolerated sparsity, and reducing the precision of the V matrix to further accelerate the AV value accumulation operation. Additionally, these methods may be adapted to decoder-only LLMs, which are very sensitive to small loss increases and do not tolerate general activation binarization. Finally, variations of this work could be explored as train-time optimizations, using binarization and sparsity to reduce the overhead of training transformer models on long sequences.

References

- [1] Dennis Abts, John Kim, Garrin Kimmell, Matthew Boyd, Kris Kang, Sahil Parmar, Andrew Ling, Andrew Bitar, Ibrahim Ahmed, and Jonathan Ross. The groq software-defined scale-out tensor streaming multiprocessor: From chips-to-systems architectural overview. In *2022 IEEE Hot Chips 34 Symposium (HCS)*, pages 1–69. IEEE Computer Society, 2022.

- [2] Anurag Arnab, Mostafa Dehghani, Georg Heigold, Chen Sun, Mario Lučić, and Cordelia Schmid. Vivit: A video vision transformer. In *Proceedings of the IEEE/CVF international conference on computer vision*, pages 6836–6846, 2021.
- [3] Iz Beltagy, Matthew E Peters, and Arman Cohan. Longformer: The long-document transformer. *arXiv preprint arXiv:2004.05150*, 2020.
- [4] Ping Chi, Shuangchen Li, Cong Xu, Tao Zhang, Jishen Zhao, Yongpan Liu, Yu Wang, and Yuan Xie. Prime: A novel processing-in-memory architecture for neural network computation in reram-based main memory. *ACM SIGARCH Computer Architecture News*, 44(3):27–39, 2016.
- [5] Mete Demircigil, Judith Heusel, Matthias Löwe, Sven Uppgang, and Franck Vermet. On a model of associative memory with huge storage capacity. *Journal of Statistical Physics*, 168:288–299, 2017.
- [6] Jia Deng, Wei Dong, Richard Socher, Li-Jia Li, Kai Li, and Li Fei-Fei. Imagenet: A large-scale hierarchical image database. In *2009 IEEE conference on computer vision and pattern recognition*, pages 248–255. Ieee, 2009.
- [7] Jacob Devlin. Bert: Pre-training of deep bidirectional transformers for language understanding. *arXiv preprint arXiv:1810.04805*, 2018.
- [8] Alexey Dosovitskiy. An image is worth 16x16 words: Transformers for image recognition at scale. *arXiv preprint arXiv:2010.11929*, 2020.
- [9] Riya Garg and Navneet Kaur. Array multiplier using xnor. *International Journal of Engineering Science and Technology (IJEST)*, 5(4):799–803, 2013.
- [10] Albert Gu and Tri Dao. Mamba: Linear-time sequence modeling with selective state spaces. *arXiv preprint arXiv:2312.00752*, 2023.
- [11] Zihan Guo and Dezhi Han. Sparse co-attention visual question answering networks based on thresholds. *Applied Intelligence*, 53(1):586–600, 2023.
- [12] Yefei He, Zhenyu Lou, Luoming Zhang, Jing Liu, Weijia Wu, Hong Zhou, and Bohan Zhuang. Bivit: Extremely compressed binary vision transformers. In *Proceedings of the IEEE/CVF International Conference on Computer Vision*, pages 5651–5663, 2023.
- [13] Itay Hubara, Matthieu Courbariaux, Daniel Soudry, Ran El-Yaniv, and Yoshua Bengio. Binarized neural networks. *Advances in neural information processing systems*, 29, 2016.
- [14] Norman P Jouppi, Cliff Young, Nishant Patil, David Patterson, Gaurav Agrawal, Raminder Bajwa, Sarah Bates, Suresh Bhatia, Nan Boden, Al Borchers, et al. In-datacenter performance analysis of a tensor processing unit. In *Proceedings of the 44th annual international symposium on computer architecture*, pages 1–12, 2017.
- [15] Jared Kaplan, Sam McCandlish, Tom Henighan, Tom B Brown, Benjamin Chess, Rewon Child, Scott Gray, Alec Radford, Jeffrey Wu, and Dario Amodei. Scaling laws for neural language models. *arXiv preprint arXiv:2001.08361*, 2020.
- [16] Nikita Kitaev, Łukasz Kaiser, and Anselm Levskaya. Reformer: The efficient transformer. *arXiv preprint arXiv:2001.04451*, 2020.
- [17] Fayez Lahoud, Radhakrishna Achanta, Pablo Márquez-Neila, and Sabine Süsstrunk. Self-binarizing networks. *arXiv preprint arXiv:1902.00730*, 2019.
- [18] Guokun Lai, Qizhe Xie, Hanxiao Liu, Yiming Yang, and Eduard Hovy. Race: Large-scale reading comprehension dataset from examinations. *arXiv preprint arXiv:1704.04683*, 2017.
- [19] In-Seok Lee, Hyeongsu Kim, Min-Kyu Park, Joon Hwang, Ryun-Han Koo, Jae-Joon Kim, and Jong-Ho Lee. Power and area-efficient xnor-and hybrid binary neural networks using tft-type synaptic devices. *IEEE Electron Device Letters*, 43(12):1912–1915, 2022.
- [20] Shuang Liang, Shouyi Yin, Leibo Liu, Wayne Luk, and Shaojun Wei. Fp-bnn: Binarized neural network on fpga. *Neurocomputing*, 275:1072–1086, 2018.
- [21] Sean Lie. Cerebras architecture deep dive: First look inside the hw/sw co-design for deep learning: Cerebras systems. In *2022 IEEE Hot Chips 34 Symposium (HCS)*, pages 1–34. IEEE Computer Society, 2022.
- [22] Liu Liu, Zheng Qu, Zhaodong Chen, Yufei Ding, and Yuan Xie. Transformer acceleration with dynamic sparse attention. *arXiv preprint arXiv:2110.11299*, 2021.
- [23] Zechun Liu, Barlas Oguz, Aasish Pappu, Lin Xiao, Scott Yih, Meng Li, Raghuraman Krishnamoorthi, and Yashar Mehdad. Bit: Robustly binarized multi-distilled transformer. *Advances in neural information processing systems*, 35:14303–14316, 2022.
- [24] Richard Yuanzhe Pang, Alicia Parrish, Nitish Joshi, Nikita Nangia, Jason Phang, Angelica Chen, Vishakh Padmakumar, Johnny Ma, Jana Thompson, He He, et al. Quality: Question answering with long input texts, yes! *arXiv preprint arXiv:2112.08608*, 2021.
- [25] Colin Raffel, Noam Shazeer, Adam Roberts, Katherine Lee, Sharan Narang, Michael Matena, Yanqi Zhou, Wei Li, and Peter J Liu. Exploring the limits of transfer learning with a unified text-to-text transformer. *Journal of machine learning research*, 21(140):1–67, 2020.
- [26] Hubert Ramsauer, Bernhard Schäfl, Johannes Lehner, Philipp Seidl, Michael Widrich, Thomas Adler, Lukas Gruber, Markus Holzleitner, Milena Pavlović, Geir Kjetil Sandve, et al. Hopfield networks is all you need. *arXiv preprint arXiv:2008.02217*, 2020.
- [27] Mohammad Rastegari, Vicente Ordonez, Joseph Redmon, and Ali Farhadi. Xnor-net: Imagenet classification using binary convolutional neural networks. In *European conference on computer vision*, pages 525–542. Springer, 2016.

- [28] Mohammad Rastegari, Vicente Ordonez, Joseph Redmon, and Ali Farhadi. XNOR-Net: Imagenet classification using binary convolutional neural networks. In *European Conference on Computer Vision (ECCV)*, pages 525–542. Springer, 2016.
- [29] Shaohuai Shi, Qiang Wang, and Xiaowen Chu. Efficient sparse-dense matrix-matrix multiplication on gpus using the customized sparse storage format. In *2020 IEEE 26th International Conference on Parallel and Distributed Systems (ICPADS)*, pages 19–26. IEEE, 2020.
- [30] Linghao Song, Yuze Chi, Atefeh Sohrabizadeh, Youngkyu Choi, Jason Lau, and Jason Cong. Sextans: A streaming accelerator for general-purpose sparse-matrix dense-matrix multiplication. In *Proceedings of the 2022 ACM/SIGDA International Symposium on Field-Programmable Gate Arrays*, pages 65–77, 2022.
- [31] Hugo Touvron, Matthieu Cord, Matthijs Douze, Francisco Massa, Alexandre Sablayrolles, and Hervé Jégou. Training data-efficient image transformers & distillation through attention. In *International conference on machine learning*, pages 10347–10357. PMLR, 2021.
- [32] A Vaswani. Attention is all you need. *Advances in Neural Information Processing Systems*, 2017.
- [33] Prateek Verma and Jonathan Berger. Audio transformers: Transformer architectures for large scale audio understanding. adieu convolutions. *arXiv preprint arXiv:2105.00335*, 2021.
- [34] Sinong Wang, Belinda Z Li, Madian Khabsa, Han Fang, and Hao Ma. Linformer: Self-attention with linear complexity. *arXiv preprint arXiv:2006.04768*, 2020.
- [35] Yuzhuang Xu, Xu Han, Zonghan Yang, Shuo Wang, Qingfu Zhu, Zhiyuan Liu, Weidong Liu, and Wanxiang Che. Onebit: Towards extremely low-bit large language models. *arXiv preprint arXiv:2402.11295*, 2024.
- [36] Zhihang Yuan, Yuzhang Shang, and Zhen Dong. Pblm: Partially binarized large language models. In *The Twelfth International Conference on Learning Representations*.
- [37] Manzil Zaheer, Guru Guruganesh, Kumar Avinava Dubey, Joshua Ainslie, Chris Alberti, Santiago Ontanon, Philip Pham, Anirudh Ravula, Qifan Wang, Li Yang, et al. Big bird: Transformers for longer sequences. *Advances in neural information processing systems*, 33:17283–17297, 2020.